Check for updates

ARTICLE

Rescue of histone hypoacetylation and social deficits by ketogenic diet in a Shank3 mouse model of autism

Luye Qin[1], Kaijie Ma[1] and Zhen Yan [1]✉

Human genetic sequencing has implicated epigenetic and synaptic aberrations as the most prominent risk factors for autism. Here we show that autistic patients exhibit the significantly lower histone acetylation and elevated HDAC2 expression in prefrontal cortex (PFC). The diminished histone acetylation is also recaptured in an autism mouse model with the deficiency of the *Shank3* gene encoding a synaptic scaffolding protein. Treating young (5-week-old) *Shank3*-deficient mice with a 4-week ketogenic diet, which can act as an endogenous inhibitor of class I HDACs via the major product β-hydroxybutyrate, elevates the level of histone acetylation in PFC neurons. Behavioral assays indicate that ketogenic diet treatment leads to the prolonged rescue of social preference deficits in *Shank3*-deficient mice. The HDAC downstream target genes encoding NMDA receptor subunits, *GRIN2A* and *GRIN2B*, are significantly reduced in PFC of autistic humans. Ketogenic diet treatment of *Shank3*-deficient mice elevates the transcription and histone acetylation of *Grin2a* and *Grin2b*, and restores the diminished NMDAR synaptic function in PFC neurons. These results suggest that the ketogenic diet provides a promising therapeutic strategy for social deficits in autism via the restoration of histone acetylation and gene expression in the brain.

INTRODUCTION

Autism spectrum disorder (ASD) is a group of neurodevelopmental disorders characterized by persistent deficits in social communication & interaction, and restricted & repetitive patterns of behavior, interests, or activities [1]. These deficits begin in early childhood and interfere with daily living throughout the lifespan. An extremely important and urgent undertaking in ASD research is to discover novel, mechanism-based interventions for this devastating mental disorder that lacks effective treatments.

Large-scale human genetic studies have revealed that many top-ranking ASD risk genes are histone-modifying enzymes and chromatin remodelers [2, 3]. One major epigenetic process regulating gene transcription is histone acetylation. The homeostasis of acetylated histone is controlled by histone acetyltransferases (HATs) and histone deacetylases (HDACs), which activate or silence gene expression via relaxing or condensing the chromatin architecture, respectively [4]. Increased HDAC expression and ensuring transcriptional dysfunction involved in synaptic transmission have been implicated in psychiatric disorders [5, 6]. A histone acetylome-wide association study also found H3K27ac aberrations at genes involved in synaptic transmission, ion transport, epilepsy, behavioral abnormality, and histone deacetylation in the prefrontal cortex (PFC) of ASD humans [7].

Haploinsufficiency of *SHANK3*, which encodes a scaffolding protein that binds to NMDA receptors and actin cytoskeleton at postsynaptic density of glutamatergic synapses [8, 9], has been linked to ASD, particularly 22q13.3 deletion syndrome (also known as Phelan-McDermid syndrome), in human genetic studies [10, 11]. Enriched ASD mutations are located at the *SHANK3*

C-terminal region (exon 21) [11], which plays a crucial role in the synaptic targeting and postsynaptic assembly of Shank3 complex. Shank3$^{+/\Delta C}$ mice with C-terminal deletion exhibit autism-like social deficits, as well as the specific loss of NMDAR synaptic function in PFC pyramidal neurons [12–16]. These abnormalities are reversed by a short treatment with class I HDAC inhibitors, such as romidepsin or MS-275 [13, 14], suggesting HDAC as a potential therapeutic target for synaptic and behavioral deficits in autism [17]. In agreement with this, our human postmortem studies have uncovered the reduced histone acetylation and elevated HDAC expression in PFC of ASD patients, which is accompanied by the diminished transcription of NMDAR genes.

An endogenous inhibitor of class I HDACs in the central nervous system, β-hydroxybutyrate [18], can be generated from a ketogenic diet, low carbohydrate and high-fat diet. It prompts us to speculate that the ketogenic diet may provide a safe and effective avenue for autism treatment. Indeed, the beneficial effects of the ketogenic diet have been reported in small-scale clinical studies of children with ASD [19, 20] and preclinical studies of various rodent models of ASD [21–24]. Here, we have revealed that ketogenic diet treatment of young Shank3-deficient mice restores NMDAR function in PFC pyramidal neurons via elevating histone acetylation and transcription of NMDAR genes, leading to the rescue of autism-related social deficits.

MATERIALS AND METHODS

Human postmortem tissues and animals

Frozen human postmortem tissues (Brodmann's area 9) from autism patients and age matched healthy controls were provided by NIH

---

[1]Department of Physiology and Biophysics, State University of New York at Buffalo, Jacobs School of Medicine and Biomedical Sciences, Buffalo, NY 14203, USA.
✉email: zhenyan@buffalo.edu

NeuroBioBank. Detailed information about these human subjects and postmortem materials is included in Sup. Fig. 1. Upon arrival, tissues were stored in a −80 °C freezer.

All experiments were performed with the approval of the Institutional Animal Care and Use Committee (IACUC) of the State University of New York at Buffalo. Mice expressing C-terminal (exon 21) deleted Shank3, Shank3$^{+/\Delta C}$ mice [25], were purchased from Jackson Laboratory and bred at our animal facility for over 7 years. Male Shank3$^{+/\Delta C}$ mice and age-matched male WT littermates were used because of the lack of social deficits in female Shank3$^{+/\Delta C}$ mice [26]. Mice were weaned at 3 weeks of age. Some mice were fed with regular control chow from Teklad Global Rodent Diets® (6.2% fat, 2018SX, Envigo, Indianapolis, IN). Other mice were switched to a ketogenic diet for 4 weeks, starting at 5-week-old (young) or 10-week-old (adult), then returned to the regular chow. The ketogenic diet [6:1 (fat: protein and carbohydrate) ratio, F3666] paste containing 75.1% fat by weight was acquired from BioServ® (Flemington, NJ). Mice with different genotypes were randomly assigned to a regular control diet or ketogenic diet. Experiments were carried out by investigators in a blinded fashion (with no prior knowledge of genotypes and treatments).

Quantitative real-time RT-PCR
Total RNA was isolated from mouse PFC punches or human postmortem tissues using Trizol reagent (Invitrogen) and treated with DNase I (Invitrogen) to remove genomic DNA. Then iScriptTM cDNA synthesis Kit (Bio-Rad) was used to obtain cDNA from the tissue mRNA. Quantitative real-time PCR was carried out using the iCycler iQ™ Real-Time PCR Detection System and iQ™ Supermix (Bio-Rad) according to the manufacturer's instructions. In brief, GAPDH was used as the housekeeping gene for quantitation of the expression of target genes in samples. Fold changes in the target genes were determined by: Fold change = $2^{-\Delta(\Delta CT)}$, where $\Delta CT = C_T$(target) $- C_T$(GAPDH), and $\Delta(\Delta C_T) = \Delta C_T$(treatment group) $- \Delta C_T$(control). For human postmortem tissues, $\Delta(\Delta C_T) = \Delta C_T$(ASD) $- \Delta C_T$(Control). C_T (threshold cycle) is defined as the fractional cycle number at which the fluorescence reaches 10x of the standard deviation of the baseline. A total reaction mixture of 20 µl was amplified in a 96-well thin-wall PCR plate (Bio-Rad) using the following PCR cycling parameters: 95 °C for 5 min followed by 40 cycles of 95 °C for 45 sec, 55 °C for 45 sec, and 72 °C for 45 sec.

Primers for human GAPDH: 5′-AGATCCCTCCAAAATCAAGT-3′ (forward), 5′-CAGAGATGATGACCCTTTTG-3′ (reverse); human HDAC1: 5′-CGGGGATGTTGGAAAATTACT-3′ (forward); 5′-CTGTGGTACTTGGTCATCTC-3′ (reverse); human HDAC2: 5′-ATCCCATGAAGCCTCATAGA-3′ (forward); 5′-TTTGTCATTTCTTCGGCAGT-3′ (reverse); human GRIN1: 5′-CCCCAAGATCGT-CAACATT-3′ (forward); 5′-ATTGAGCTGAATCTTCCAGG-3′ (reverse); human GRIN2A: 5′-AGAGTGGGCTATTGGACC-3′ (forward); 5′- GCATCACCGCAA-TATTTAGC-3′ (reverse); human GRIN2B: 5′-CATTGGCATTGCTGTCATC-3′ (forward); 5′-GGTCTCATTCATGGCTACC-3′ (reverse). Primers for mouse Grin1: 5′-CATCGGACTTCAGCTAATCA-3′ (forward); 5′-GTCCCCATCCTCATT-GAATT-3′ (reverse); mouse Grin2a: 5′-GGCTACAGAGACTTCATCAG-3′ (forward); 5′-ATCCAGAAGAAATCGTAGCC-3′ (reverse); mouse Grin2b: 5′-TTAACAACTCCGTACCTGTG-3′ (forward); 5′- TGGAACTTCTTGTCACTCAG-3′ (reverse); mouse Gapdh: 5′-GACAACTCACTCAAGATTGTCAG-3′ (forward); 5′-ATGGCATGGACTGTGGTCATGAG-3′ (reverse).

Western blotting of nuclear, synaptic and total proteins
Nuclear extracts from human postmortem tissues were prepared according to the manufacturer's instructions (Life Technologies) with modifications. Briefly, PFC punches of human postmortem tissues were collected, and then homogenized with 500 µl hypotonic buffer (20 mM Tris-HCl, pH 7.4, 10 mM NaCl, 3 mM MgCl₂, 0.5% NP-40, 1 mM PMSF, with cocktail protease inhibitor). The homogenate was incubated on ice for 15 min and followed by centrifugation at 3,000 g, 4 °C for 10 min. The nuclear pellet was resuspended in 50 µl nuclear extract buffer (100 mM Tris-HCl, pH 7.4, 100 mM NaCl, 1 mM EDTA, 1% Triton X-100, 0.1% SDS, 10% glycerol, 1 mM PMSF, with cocktail protease inhibitor) and incubated on ice for 30 min with periodic vortexing to resuspend the pellet. After centrifugation, the supernatant for nuclear fractions was collected, boiled in 2 × SDS loading buffer for 5 min and then separated on 6% or 12% SDS-polyacrylamide gels. Western blotting experiments for nuclear proteins were performed with antibodies against H3K9ac (1:1,000, Cell Signaling, 9649), H3 (1:500, Cell Signaling Technology, 4499), HDAC1 (1:500, Cell Signaling, 34589), or HDAC2 (1:500, Cell Signaling, 57156).

Synaptic membrane fractions were prepared as described previously [12, 14]. In brief, PFC punches of human postmortem tissues were collected and homogenized in ice-cold lysis buffer (10 mL/g, 15 mM Tris, pH 7.6, 0.25 M sucrose, 1 mM PMSF, 2 mM EDTA, 1 mM EGTA, 10 mM Na₃VO₄, 25 mM NaF, 10 Mm sodium pyrophosphate and protease inhibitor tablet). After centrifugation at 800 g for 5 min to remove nuclei and large debris, the remaining supernatant was subjected to 10,000 g centrifugation for 10 min. The crude synaptosome fraction (pellet) was suspended in lysis buffer containing 1% Triton X-100 and 300 mM NaCl, homogenized again and centrifuged at 16,000 g for 15 min. The Triton insoluble fraction, which mainly includes membrane-associated proteins from synaptosomes, was dissolved in 1% SDS. Samples were boiled in 2 × SDS loading buffer for 5 min and separated on 7.5% SDS-PAGE.

For the extraction of total proteins in immunoblotting, the modified radioimmunoprecipitation assay buffer (1% Triton X-100, 0.1% SDS, 0.5% deoxycholic acid, 50 mM NaPO4, 150 mM NaCl, 2 mM EDTA, 50 mM NaF, 10 mM sodium pyrophosphate, 1 mM sodium orthovanadate, 1 mM phenylmethylsulfonyl fluoride, and 1 mg/ml leupeptin) was used.

Western blotting of synaptic or total proteins was performed using antibodies against NR1 (1:500, NeuroMab, 75-272), NR2A (1:500, Millipore, 07-632), NR2B (1:500, Millipore, 06-600) and PSD-95 (1:1000, Cell Signaling, 36233).

Immunohistochemistry
Mice were anesthetized and transcardially perfused with PBS, followed by 4% paraformaldehyde before brain removal. Brains were post-fixed in 4% PFA overnight and cut into 100 µm slices coronally. Slices were washed and blocked for 1 h in PBS containing 5% BSA and 0.05% Triton. After washing, slices were incubated with the primary antibody against acetylated H3K9 (1:1,000, Cell Signaling, 9649) and NeuN (1:1000, Millipore, MAB377) or CaMKII (1:500, Abcam, ab22609) overnight at 4 °C. After washing three times in PBS, slices were incubated with secondary antibodies (Alexa Fluor 594, Invitrogen A11037) for 1 h at room temperature, followed by three washes with PBS. Slices were mounted on slides with Vectashield mounting media (Vector Laboratories). Images were acquired using a 63 × objective on a Leica TCS SP8 confocal microscope. All specimens were imaged under identical conditions and analyzed with identical parameters using Image J software.

β-hydroxybutyrate analysis
The prefrontal cortex was dissected from the mouse brain, and the level of β-hydroxybutyrate was measured using a β-hydroxybutyrate assay kit (Sigma, MAK041) as instructed by the manufacturer. In this assay, β-hydroxybutyrate concentration is determined by a coupled enzyme reaction, which results in a colorimetric (450 nm) product, proportional to the level of β-hydroxybutyrate.

Chromatin immunoprecipitation (ChIP)
Briefly, PFC punches from mouse slices were collected. Each sample was homogenized in 250 µl ice-cold douncing buffer (10 mM Tris-HCl, pH 7.5, 4 mM MgCl₂,1 mM CaCl₂). The homogenized sample was incubated with 12.5 µl micrococcal nuclease (5 U/ml, Sigma, N5386) for 7 min and terminated by adding EDTA at a final concentration of 10 mM. Then hypotonic lysis buffer (1 ml) was added and incubated on ice for 1 hr. The supernatant was transferred to a new tube after centrifugation. After adding 10× incubation buffer (50 mM EDTA, 200 mM Tris-HCl, 500 mM NaCl), 10% of the supernatant was saved to serve as input control. To reduce nonspecific background, the supernatant was pre-cleared with 100 µl of salmon sperm DNA/protein A agarose 50% slurry (Millipore, 16–157) for 2 hr at 4 °C with agitation. The pre-cleared supernatant was incubated with pan-acetylated H3 antibody (Millipore, 06-599) overnight at 4 °C under constant rotation, followed by incubation with 60 µl of salmon sperm DNA/Protein A agarose 50% Slurry for 2 hr at 4 °C. After washing five times, the bound complex was eluted twice from the beads by incubating with the elution buffer (100 µl) at room temperature. Proteins and RNA were removed by using proteinase K (Invitrogen) and RNase (Roche). Then immunoprecipitated DNA and input DNA were purified by QIAquick PCR purification Kit (Qiagen). Quantification of ChIP signals was calculated as percent input. Purified DNA was subjected to qPCR reactions with primers against mouse Grin1 promoter (Forward, 371 bp to 390 bp relative to TSS, 5′-CAGTAAACCAGGCCAATAAG-3′; Reverse, 566 – 585 bp relative to TSS, 5′-AGGAGACTGAGAAGGACCAG-3′), Grin2a promoter (Forward, −273 – −254 bp relative to TSS, 5′-GCCACTGCTGAGAACTATGT-3′; Reverse, −56–37 bp relative to TSS, 5′-CTGGCTGAGTTTGCTATGAG-3′), Grin2b promoter (Forward, −436 – −417 bp relative to TSS, 5′-ACTCACTGGCGAGTTAAGTG-3′; Reverse, −247– −228 bp relative to TSS, 5′-ATAATTCCGAAAAGGTCTGC-3′).

Electrophysiological recordings of brain slices

The whole-cell voltage-clamp recording technique was used to measure synaptic currents in layer five pyramidal neurons of prefrontal cortical slices, as previously described [12, 14]. Mouse slices (300 μm) were positioned in a perfusion chamber attached to the fixed stage of an upright microscope (Olympus) and submerged in continuously flowing oxygenated ACSF (in mM: 130 NaCl, 26 NaHCO$_3$, 1 CaCl$_2$, 5 MgCl$_2$, 3 KCl, 1.25 NaH$_2$PO$_4$, 10 glucose, pH 7.4, 300 mOsm). Layer V medial PFC pyramidal neurons were visualized with a 40X water-immersion lens and recorded with the Multiclamp 700 A amplifier (Molecular Devices, Sunnyvale, CA).

Bicuculline (20 μM) and CNQX (20 μM) were added in NMDAR-EPSC recordings. Patch electrodes contained the following internal solution (in mM): 130 Cs-methanesulfonate, 10 CsCl, 4 NaCl, 10 HEPES, 1 MgCl$_2$ 2 QX-314, 12 phosphocreatine, 5 MgATP, 0.2 Na$_3$GTP, 0.1 leupeptin, pH 7.2–7.3, 265–270 mOsm. Evoked synaptic currents were generated with a pulse from a stimulation isolation unit controlled by an S48 pulse generator (Grass Technologies, West Warwick, RI). A bipolar stimulating electrode (FHC, Bowdoinham, ME) was placed ~100 μm from the neuron under recording. For NMDAR-EPSC, the cell (clamped at –70 mV) was depolarized to + 40 mV for 3 s before stimulation to fully relieve the voltage-dependent Mg^{2+}. For input-output responses, the synaptic current was elicited by a series of pulses with different stimulation intensities (50–90 μA) delivered at 0.05 Hz.

Behavioral testing

Social preference test. A three-chamber social interaction assay was performed to assess social deficits [12, 14, 26]. Briefly, an apparatus (L: 101.6 cm, W: 50.8 cm, H: 50.8 cm) containing three chambers with retractable doorways allowing for access to side chambers was used. Animals were habituated in the apparatus for one day before testing. During the habituation, two empty capsules (inverted pencil cup, D: 10.2 cm, H: 10.5 cm) were placed in the side chambers, and an upright cup was placed on top of each capsule to prevent the subject mouse from climbing on top. Animals were allowed to explore all 3 chambers of the apparatus for 10 min. The test was composed of two phases with different stimuli in each of the side chambers. The 1st phase contained two identical nonsocial stimuli (folded papers), the 2nd phase contained a nonsocial (NS) stimulus (a woodblock) and a social (Soc) stimulus (an age- and sex-matched wild-type mouse of the same strain). Each stimulus was placed inside a capsule placed in the side chamber. The test animal was placed in the center chamber, and was free to explore the apparatus for 10 min in each phase, while it was returned to the home cage during the 10-min intervals between phases. The chamber was cleaned with 75% Ethanol after each phase. Interaction time was counted based on "investigating" behaviors of the test animal to each stimulus. A computer running the Any-maze tracking software (Stoelting, Wood Dale, IL) measured the time of the test animal spent at the close proximity of the capsule (distance of animal head to cup edge: ≤ 3.5 cm). Preference index scores were calculated, where time spent with one stimulus was subtracted from the time spent with the other stimulus and divided by the total time spent exploring both stimuli.

Self-grooming. Mice were scored for spontaneous grooming behaviors when placed individually in a clean cage. The cage was lined with a thin layer of bedding (~1 cm) in order to reduce neophobia but prevent digging, a potentially competing behavior. Prior to the testing period, animals were allowed to habituate to the novel environment for 10 min. Each mouse was rated for 10 min on cumulative time spent grooming.

Open field test. Animals were placed on an apparatus (L: 67.7 cm, W: 50.8 cm, H: 50.8 cm) to move freely for 10 min. The total distance traveled and the amount of time the animal spent in the center (33.8 cm × 25.4 cm) was counted by Any-maze tracking software (Stoelting, Wood Dale, IL). Anxious animals spend less time in the center and more time in the corner of the field.

Rotarod test. To assess motor coordination and balance, an accelerating rotarod (San Diego Instruments, San Diego CA) was used. Mice were placed on a cylinder, which slowly accelerated from 4 to 40 r.p.m. over a 5-min test session. The task requires mice to walk forward in order to remain on top of the rotating cylinder rod.

Statistical analysis

Data were analyzed with GraphPad Prism 7 (GraphPad), Clampfit (Molecular Devices, Sunnyvale, CA), and Mini analysis (Synaptosoft, NJ). No samples were excluded from analyses. Normality and equivalence of variance were checked for each data set. Differences between two groups were assessed with an unpaired two-tailed Student's *t*-test. Differences between more than two groups were assessed with one-way or two-way ANOVA, followed by post hoc Bonferroni tests for multiple comparisons. All values are means ± SEM.

RESULTS

ASD humans exhibit significantly decreased histone acetylation and increased HDAC2 expression in PFC

To elucidate the role of histone acetylation in ASD, we examined the global histone 3 acetylation in human postmortem tissue of the PFC (Brodmann's area 9) from idiopathic ASD patients vs. age and sex-matched control subjects. As shown in Fig. 1A, the level of H3 lysine 9 acetylation (H3K9ac) in the nuclear fraction of PFC lysates from ASD patients was significantly decreased compared to controls. Immunostaining of H3K9ac and NeuN (a neuronal marker) also showed that the fluorescent signal intensity of H3K9ac in PFC neurons (NeuN +) from ASD patients was significantly lower than control subjects (Fig. 1B, C).

To find out the HDAC family members that may mediate the lower histone acetylation level in ASD humans, we examined the expression of HDAC2, which is crucial for controlling brain development [27], and HDAC1. As shown in Fig. 1D, E, the mRNA and protein levels of HDAC2, but not HDAC1, were significantly higher in PFC of ASD patients than control subjects, which may contribute to the decreased histone acetylation.

Shank3-deficient mice have decreased histone acetylation in PFC neurons, which is reversed by ketogenic diet treatment

Consistent with the ASD human data, Shank3$^{+/ΔC}$ mice also exhibit the elevated HDAC2 expression and reduced histone acetylation in PFC [13, 14]. Prior studies have shown that β-hydroxybutyrate, the major product of the ketogenic diet, can act as an endogenous inhibitor of class I HDACs in the CNS [18] [23]. So we examined the effect of the ketogenic diet on the level of histone acetylation in *Shank3*-deficient mice. Male Shank3$^{+/ΔC}$ mice (5-week-old) and age-matched WT mice were subjected to a 4-week regimen of a ketogenic diet or regular control diet before testing. The level of β-hydroxybutyrate in the brain (PFC) of both WT and Shank3$^{+/ΔC}$ mice was significantly elevated by the ketogenic diet (Fig. 2A). The fluorescence intensity of H3K9ac in PFC pyramidal neurons (CaMKII +) was significantly lower in Shank3$^{+/ΔC}$ mice than WT mice (with control diet), which was significantly elevated in ketogenic diet-treated Shank3$^{+/ΔC}$ mice (Fig. 2B, C), indicating the effectiveness of this dietary treatment in restoring histone acetylation in the brain of *Shank3*-deficient mice.

Ketogenic diet rescues autism-like social deficits in *Shank3*-deficient mice

Next, we examined the effect of a ketogenic diet on social deficits in young male Shank3$^{+/ΔC}$ mice, which exhibit the impaired social preference in the three-chamber social interaction assay [12] [13, 14, 28] a commonly used approach to measure sociability [26]. As shown in Fig. 3A, B, during the presentation of both social (Soc) and nonsocial (NS) stimuli, ketogenic diet-treated Shank3$^{+/ΔC}$ mice spent significantly more time exploring the Soc stimulus over the NS object, similarly to WT mice, while control diet-treated Shank3$^{+/ΔC}$ mice had a significant loss of the preference for the Soc stimulus. WT mice treated with a ketogenic diet had unchanged social preferences. The significantly elevated social preference index in *Shank3*-deficient mice subjected to a ketogenic diet (Fig. 3C) indicates that this dietary treatment alleviates the observed social deficits.

To determine how long the rescue effect of ketogenic diet could last, social preference assays were performed in Shank3$^{+/ΔC}$ mice before and at various time points after 4 weeks' ketogenic diet treatment. The significantly increased social preference index
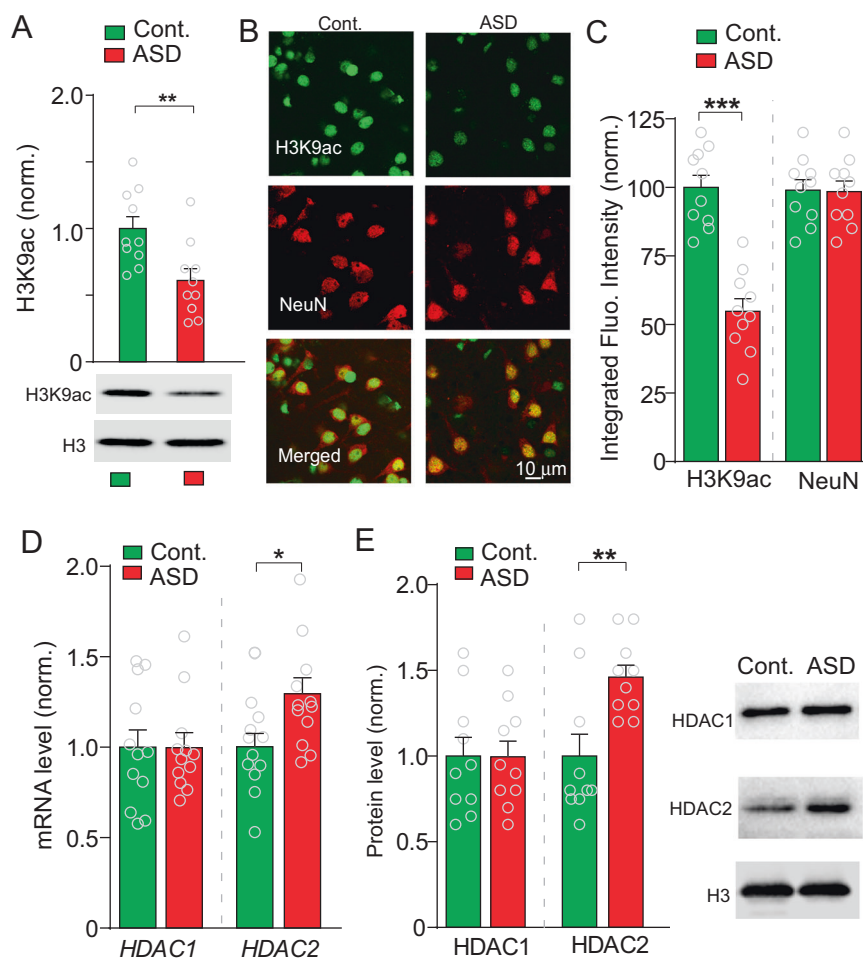
Fig. 1 Significantly decreased histone acetylation and increased HDAC2 expression are found in PFC of autistic humans. A Immunoblots and quantification analysis of the level of acetylated histone 3 (H3K9ac) and total histone 3 (H3) in the nuclear fraction of postmortem tissue of PFC (Brodmann's Area 9) from idiopathic ASD patients vs. age and sex-matched control subjects ($n = 10$/group, $t_{18} = 3.1$, **$p < 0.01$, t-test). **B, C** Confocal images (**B**) and quantification (**C**) of H3K9ac and NeuN immunohistochemical signals in PFC neurons from human control subjects and ASD patients ($n = 10$ slices/3 humans/group, $t_{18} = 7.01$, ***$p < 0.001$, t-test). **D** Quantitative real-time RT-PCR data on *HDAC1* and *HDAC2* mRNAs in PFC of human control subjects and ASD patients ($n = 12$/group, $t_{22} = 2.45$, *$p < 0.05$, t-test). **E** Immunoblots and quantitative analysis of HDAC1 and HDAC2 proteins in the nuclear fraction of PFC from human control subjects and ASD patients ($n = 10$/group, $t_{18} = 3.17$, **$p < 0.01$, t-test).

in *Shank3*-deficient mice persisted for at least 6 weeks post-treatment of the ketogenic diet, while no improvement in social preference was found with repeated measurements of control diet—treated Shank3$^{+/\Delta C}$ mice (Fig. 3D).

We further examined the effect of the ketogenic diet on social approach behaviors in young male Shank3$^{+/\Delta C}$ mice. Compared to WT mice, Shank3$^{+/\Delta C}$ mice spent significantly less time approaching and interacting with social stimuli, which was almost completely reversed by ketogenic diet treatment (Fig. 3E, F). Taken together, these results suggest that ketogenic diet treatment can effectively rescue autism-like social deficits in the *Shank3*-deficient model.

A variety of other behaviors were also examined. The ketogenic diet failed to normalize the increased repetitive grooming in Shank3$^{+/\Delta C}$ mice (Fig. 3G). No differences were observed between WT and Shank3$^{+/\Delta C}$ mice treated with ketogenic diet or control diet in rotarod, locomotion, and open field tests (Fig. 3H–J), suggesting that ketogenic diet does not affect motor coordination or anxiety-like behavior.

ASD is a lifelong disorder. To find out whether ketogenic diet can have similar therapeutic effects in adulthood, we treated adult (10-week-old) male Shank3$^{+/\Delta C}$ mice with ketogenic diet for 4 weeks and assessed their sociability. As shown in Fig. 3K,

ketogenic diet-treated adult Shank3$^{+/\Delta C}$ mice had the significantly increased social preference index, compared to control diet-treated adult Shank3$^{+/\Delta C}$ mice, which persisted for 2 weeks post-treatment. The shorter effect of ketogenic diet in adult Shank3$^{+/\Delta C}$ mice suggests that the therapeutic efficacy of HDAC inhibition is influenced by developmental processes.

NMDAR transcription and synaptic expression are diminished in ASD humans

To find out the potential gene targets of HDAC that are involved in the therapeutic effects of the ketogenic diet, we focused on NMDA receptors because glutamatergic dysfunction has been linked to social deficits in autism models with the loss of Shank family members [25, 29–35]. We first examined the expression of NMDA receptor subunits in human postmortem tissues. Quantitative PCR analyses (Fig. 4A) showed the significantly decreased *GRIN2A* (encoding NR2A subunit) and *GRIN2B* (encoding NR2B subunit), but not *GRIN1* (encoding NR1 subunit), in PFC of ASD patients. Consistently, the level of NR2A and NR2B, but not NR1, in the synaptic fraction of ASD PFC was significantly decreased, compared to control subjects (Fig. 4B). These results suggest the diminished NMDAR function in PFC of ASD patients.
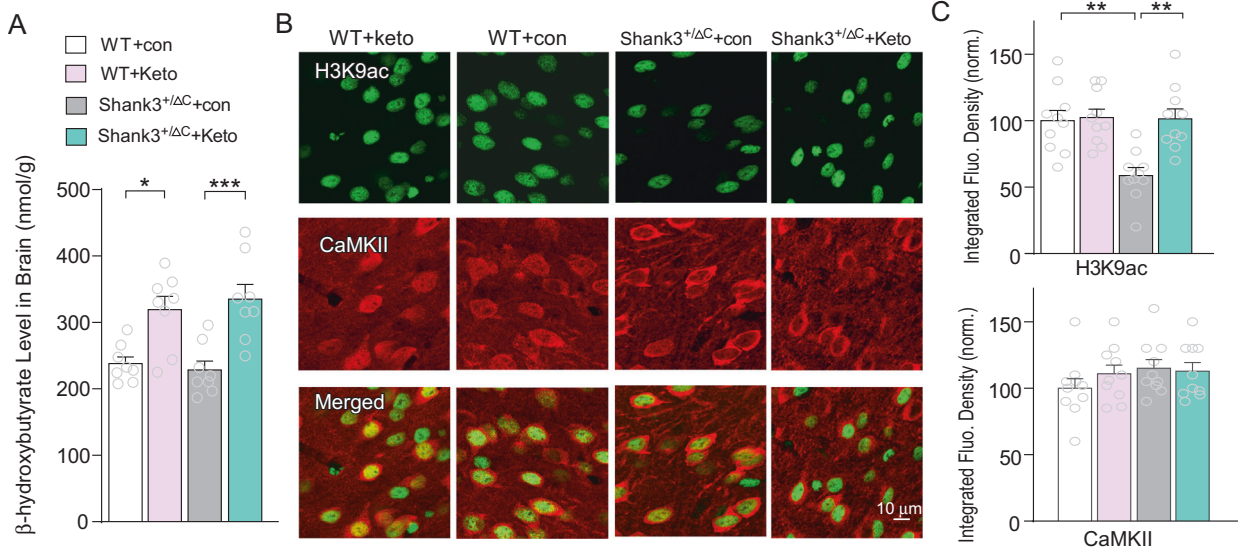
Fig. 2 Ketogenic diet restores the diminished histone acetylation in *Shank3*-deficient mice. A Bar graphs showing the level of β-hydroxybutyrate in the brain of WT or Shank3$^{+/\Delta C}$ mice treated with 4-week regular control diet (con) or ketogenic diet (Keto) ($n = 8$/group, $F_{1,28(treatment)} = 29.86$, $p < 0.0001$, two-way ANOVA). **B, C** Confocal images (**B**) and quantification (**C**) of H3K9ac and CaMKII immunohisto-chemical signals in PFC neurons from WT or Shank3$^{+/\Delta C}$ mice treated with con or Keto diet ($n = 10$ images/4 mice/group. $F_{1,36(treatment)} = 10.51$, $p = 0.0026$; $F_{1,36(genotype)} = 9.24$, $p = 0.0044$, **$p < 0.01$, two-way ANOVA).

Ketogenic diet elevates NMDAR transcription and histone acetylation, and restores NMDAR function in *Shank3*-deficient mice

Next, we examined whether ketogenic diet could elevate NMDAR expression and function in PFC of Shank3$^{+/\Delta C}$ mice. Quantitative PCR analyses (Fig. 5A) showed that the mRNA level of *Grin2a* and *Grin2b*, but not *Grin1*, was significantly elevated in young Shank3$^{+/\Delta C}$ mice treated with 4-week ketogenic diet. Western blotting also indicated the significantly increased NR2A and NR2B protein levels in ketogenic diet-treated Shank3$^{+/\Delta C}$ mice, compared to those administered with the control diet (Fig. 5B).

To determine the role of histone acetylation in the increased *Grin2a* and *Grin2b* transcription by the ketogenic diet, we performed ChIP assays to examine the histone acetylation at the promoter region of NMDAR subunits. As shown in Fig. 5C, the ketogenic diet significantly increased H3 acetylation at *Grin2a* and *Grin2b* promoters in Shank3$^{+/\Delta C}$ mice. No significant effect was observed on H3 acetylation at *Grin1* promoter. These data suggest that the ketogenic diet increases *Grin2a* and *Grin2b* transcription by enhancing their histone acetylation in Shank3$^{+/\Delta C}$ mice.

To find out whether the upregulated *Grin2a* and *Grin2b* expression by ketogenic diet could restore the diminished NMDAR function in Shank3$^{+/\Delta C}$ mice, we performed electrophysiological experiments to record NMDAR-mediated excitatory postsynaptic currents (NMDAR-EPSC) after 4-week ketogenic diet treatment. Layer five pyramidal neurons in PFC, which show the clearest deficits in postmortem tissue from autistic children [36], were selected for recordings. As shown in Fig. 5D, the amplitude of NMDAR-EPSC induced by a series of stimulus intensities was significantly elevated in ketogenic diet-treated Shank3$^{+/\Delta C}$ mice, compared to control diet-treated Shank3$^{+/\Delta C}$ mice. The restoration of NMDAR function may underlie the rescue of social deficits in *Shank3*-deficient mice with ketogenic diet treatment.

DISCUSSION

In this study, we have revealed the reduced histone acetylation and increased HDAC2 expression in postmortem tissue of PFC from idiopathic ASD patients, which prompts us to explore the therapeutic potential of HDAC inhibition in autism. Using the Shank3-deficient model of autism, which exhibit the similar aberration of histone acetylation [14], we have found that 4-week ketogenic diet treatment elevates histone acetylation in PFC and induces the prolonged rescue of social preference deficits in Shank3$^{+/\Delta C}$ mice. Consistently, significantly improved core features (sociability) were observed in small population clinical studies of children with ASD [19, 20].

Ketogenic diet has been well established as a remarkably effective nonpharmacological treatment for epilepsy and even drug-refractory seizures [37]. Ketogenic diet rescues hippocampal memory defects in a mouse model of Kabuki syndrome [23], reduces midlife mortality, extends longevity and improves memory in aging mice [38, 39]. Prior studies have found that ketogenic diet increases sociability in several autism-associated mouse models, including BTBR mice [22], the prenatal valproic acid (VPA) rodent model of ASD [21], Engrailed 2 null mice [40], and a maternal immune activation model of ASD [24], suggesting the therapeutic potential of the ketogenic diet in autism. While the modification of gut microbiota, mitochondrial function, and excitation-inhibition balance has been implicated in the beneficial effects of ketogenic diet [21, 41–43], the underlying molecular mechanisms causally link ketogenic diet to neuronal communication and social behaviors remain elusive.

The ketogenic diet generates β-hydroxybutyrate, the natural end product of hepatic fatty acid beta oxidation [44], which is able to be actively transported into the CNS to inhibit class I HDACs and suppress oxidative stress [18]. Our current study suggests that the ketogenic diet ameliorates social deficits in *Shank3*-deficient mice via inhibiting HDAC and elevating histone acetylation in PFC, similar to the therapeutic effects of class I HDAC inhibitors in Shank3$^{+/\Delta C}$ mice [13, 14, 45]. A striking feature of ketogenic diet treatment is the long-lasting effect on social deficits in young mice (at least 6 weeks) and even in adult mice (2 weeks), providing a highly safe and powerful avenue for autism treatment.

HDAC2 is enriched at the promoters of genes implicated in synaptic remodeling/plasticity or regulated by neuronal activity, including NMDAR subunits *Grin2a*, *Grin2b*, *Bdnf*, *Egr1*, *Fos*, and *Camk2a* [46]. NMDAR-mediated synaptic dysfunction is strongly implicated in ASD, because loss-of-function mutations in genes encoding NMDAR subunits (e.g., *GRIN2B*) and their regulators (e.g. *SHANK3*) are top-ranking autism risk factors [2, 3]. Consistently, we
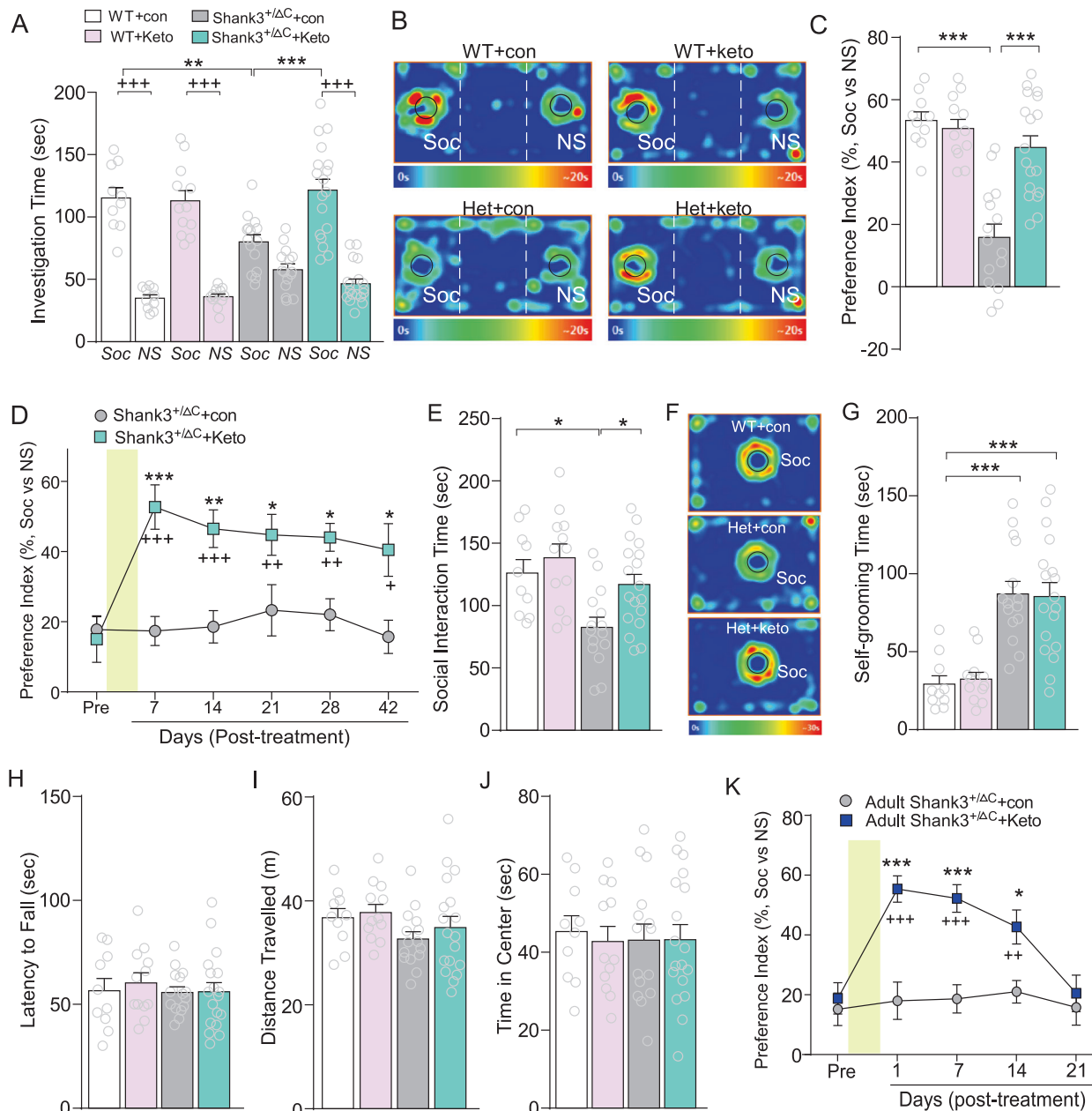
Fig. 3 Ketogenic diet ameliorates autism-like social deficits in *Shank3*-deficient mice. A, B Plots showing the time spent investigating either the social (Soc) or nonsocial (NS) stimulus (**A**) and the social preference index (**B**) during three-chamber sociability testing in young male WT and Shank3$^{+/\Delta C}$ mice treated with regular diet (con) or ketogenic diet (Keto) ($n = 10$–18/group, $F_{1,51} = 16.79$, $p = 0.0001$, **$p < 0.01$, ***$p < 0.001$, con vs. Keto; +++$p < 0.001$, pre- vs. post-treatment, two-way ANOVA). **C** Representative heat maps illustrating the time spent in different locations of the 3 chambers (blue: 0 sec; red: ~ 20 sec). Locations of Soc and NS stimuli are labeled with the circles. **D** Plots of social preference index in young Shank3$^{+/\Delta C}$ mice treated with con vs. Keto diet at different time points ($n = 8$–9/group, $F_{1,15(treatment)} = 32.96$, $p < 0.001$. *$p < 0.05$, *$p < 0.01$, ***$p < 0.001$, con vs. Keto; +$p < 0.05$, ++$p < 0.01$, +++$p < 0.001$, pre- vs. post-treatment, two-way repeated measures ANOVA). **E** Plots showing total social interaction time during social approach tests in young WT and Shank3$^{+/\Delta C}$ mice treated with con vs. Keto diet ($n = 10$–18/group, $F_{1,51} = 5.96$, $p = 0.018$, *$p < 0.05$, two-way ANOVA). **G–J** Plots showing a variety of behaviors in young WT and Shank3$^{+/\Delta C}$ mice treated with con vs. Keto diet, including the time spent self-grooming (**G**), the latency to fall during rotarod tests (**H**), the total distance traveled (**I**), and the time spent in the center during open field tests (**J**) ($n = 10$–18/group, G: $F_{1,51(treatment)} = 0.009$, $p = 0.93$, $F_{1,51(genotype)} = 47.52$, ***$p < 0.001$, two-way ANOVA). **K** Plots of social preference index in adult Shank3$^{+/\Delta C}$ mice treated with con vs. Keto diet at different time points ($n = 9$–10/group, $F_{1,17(treatment)} = 49.19$, $p < 0.001$, *$p < 0.05$, ***$p < 0.001$, con vs. Keto; ++$p < 0.01$, +++$p < 0.001$, pre-vs. post-treatment, two–way repeated measures ANOVA).

have revealed the diminished transcription of *GRIN2A* and *GRIN2B* subunits, as well as the reduced level of synaptic NR2A and NR2B subunits in the postmortem tissue of PFC from idiopathic ASD patients, suggesting the loss of NMDAR function in autistic humans.

The causal involvement of NMDARs in autistic phenotypes is also demonstrated by preclinical studies showing that restoring

NMDAR function ameliorates social deficits in ASD mouse models [12–15, 47–49]. *Shank3*-deficient mice have unchanged mRNA levels and total protein levels of NMDARs. However, they exhibit the reduced level of synaptic NMDARs and NMDAR hypofunction in PFC pyramidal neurons due to the loss of actin-based synaptic delivery of NMDARs [12, 14]. Here we show that the ketogenic diet
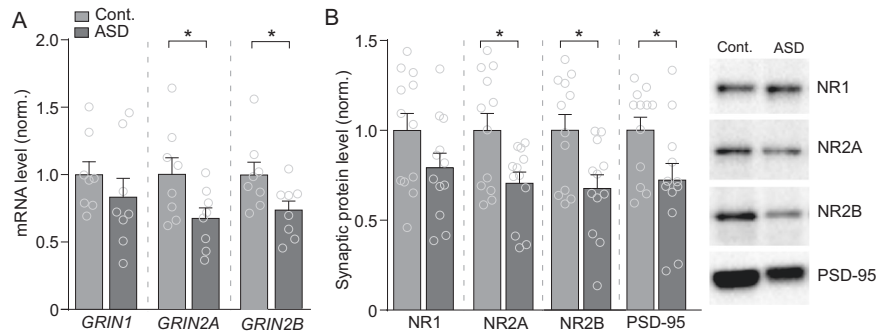
Fig. 4 Diminished NMDAR transcription and synaptic expression are found in PFC of autistic humans. A Quantitative real-time RT-PCR data on *GRIN1*, *GRIN2A* and *GRIN2B* mRNAs in postmortem tissue of PFC (Brodmann's Area 9) from idiopathic ASD patients vs. age and sex-matched control subjects ($n = 8$/group, *GRIN2A*: $t_{14} = 2.24$; *GRIN2B*: $t_{14} = 2.25$, $*p < 0.05$, t-test). **B** Immunoblots and quantitative analysis of NR1, NR2A, NR2B, and PSD-95 in the synaptic fraction of PFC from human control subjects and ASD patients ($n = 12$/group, NR2A: $t_{22} = 2.62$; NR2B: $t_{22} = 2.78$; PSD_95: $t_{22} = 2.38$, $*p < 0.05$, t-test).
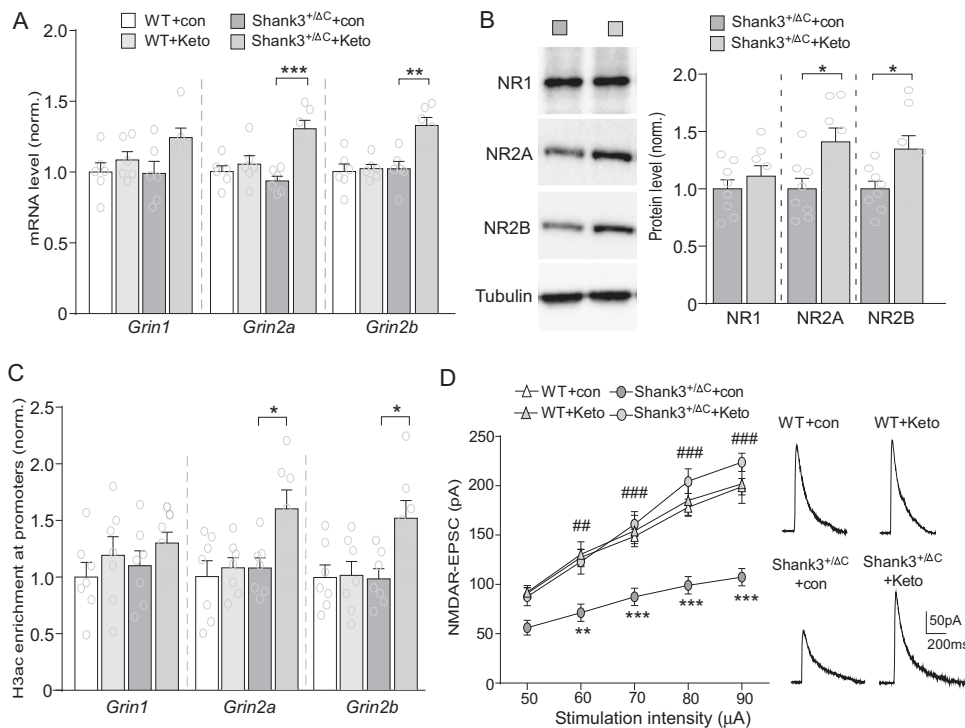

Fig. 5 Ketogenic diet elevates the transcription and histone acetylation of NMDAR subunits, and restores NMDAR function in PFC of young *Shank3*-deficient mice. A Quantitative real-time PCR data on the mRNA level of NMDAR subunits in PFC slices from WT and Shank3$^{+/\Delta C}$ mice treated with con vs. Keto diet ($n = 6$/group, *Grin2a*: $F_{1,20(treatment)} = 17.34$, $p = 0.0005$; *Grin2b*: $F_{1,20(treatment)} = 10.92$, $p = 0.0035$, $**p < 0.01$; $***p < 0.001$; two-way ANOVA). **B** Immunoblots and quantitative analysis of NR1, NR2A, and NR2B in Shank3$^{+/\Delta C}$ mice treated with con vs. Keto diet ($n = 8$/group, NR1: $t_{14} = 0.92$, $p = 0.38$; NR2A: $t_{14} = 2.73$, $*p < 0.05$; NR2B: $t^{14} = 2.58$, $*p < 0.05$, t-test). **C** ChIP assay data showing the acetylated histone H3 (H3ac) level at *Grin1*, *Grin2a*, and *Grin2b* promoter regions in PFC lysates from WT and Shank3$^{+/\Delta C}$ mice treated with con vs. keto diet ($n = 7$/group. *Grin1*: $F_{1,24(treatment)} = 2.18$, $p = 0.15$; *Grin2a*, $F_{1,24(treatment)} = 5.63$, $*p < 0.05$; *Grin2b*, $F_{1,24(treatment)} = 5.16$, $*p < 0.05$; two-way ANOVA). **D** Input-output curves of the NMDAR-EPSC in PFC pyramidal neurons from WT and Shank3$^{+/\Delta C}$ mice treated with con vs. Keto diet ($n = 12$ cells/3 mice/group, $F_{3,44(treatment)} = 12.81$, $p < 0.0001$, $**p < 0.01$, $***p < 0.001$, WT+con vs. Shank3$^{+/\Delta C}$ + con; $\#\#p < 0.01$, $\#\#\#p < 0.001$, Shank3$^{+/\Delta C}$ + con vs. Shank3$^{+/\Delta C}$ + Keto, two-way repeated measures ANOVA). Inset: representative NMDAR-EPSC traces.

elevates the transcription of NMDAR subunits (*Grin2a and Grin2b*) via increasing the histone acetylation at their promotors, similar to the effects of class I HDAC inhibitors [13, 14]. It provides an avenue to compensate for the loss of synaptic NMDARs in Shank3$^{+/\Delta C}$ mice, which is reflected by the restoration of NMDAR-mediated synaptic function in PFC pyramidal neurons. Taken together, these results have offered a scientific basis for using a ketogenic diet as a novel treatment approach for ASD patients.

While our findings in a *Shank3* model of autism are consistent with the promising results from preclinical studies of ASD models and clinical studies of autistic children, one limitation of the ketogenic diet is the low compliance in some human patients, probably because the diet causes or increases gastrointestinal disturbances. Given the huge heterogeneity of ASD and the small percentage of ASD involving *Shank3* haploinsufficiency, another limitation is that the ketogenic diet may not work in all ASD cases. Future studies will examine the general applicability of the ketogenic diet in treating autism linked to various genetic mutations.

DATA AVAILABILITY
All data are available upon request.

REFERENCES

1. Yenkoyan K, Grigoryan A, Fereshetyan K, Yepremyan D. Advances in understanding the pathophysiology of autism spectrum disorders. Behav Brain Res. 2017;331:92–101.

2. De Rubeis S, He X, Goldberg AP, Poultney CS, Samocha K, Cicek AE, et al. Synaptic, transcriptional and chromatin genes disrupted in autism. Nature 2014;515:209–15.

3. Satterstrom FK, Kosmicki JA, Wang J, Breen MS, De Rubeis S, An JY, et al. Large-scale exome sequencing study implicates both developmental and functional changes in the neurobiology of autism. Cell 2020;180:568–84. e23

4. Bannister AJ, Kouzarides T. Regulation of chromatin by histone modifications. Cell Res. 2011;21:381–95.

5. Abel T, Zukin RS. Epigenetic targets of HDAC inhibition in neurodegenerative and psychiatric disorders. Curr Opin Pharm. 2008;8:57–64.

6. Grayson DR, Kundakovic M, Sharma RP. Is there a future for histone deacetylase inhibitors in the pharmacotherapy of psychiatric disorders? Mol Pharm. 2010;77:126–35.

7. Sun W, Poschmann J, Cruz-Herrera Del Rosario R, Parikshak NN, Hajan HS, Kumar V, et al. Histone acetylome-wide association study of autism spectrum disorder. Cell 2016;167:1385–97. e11

8. Naisbitt S, Kim E, Tu JC, Xiao B, Sala C, Valtschanoff J, et al. Shank, a novel family of postsynaptic density proteins that binds to the NMDA receptor/PSD-95/GKAP complex and cortactin. Neuron 1999;23:569–82.

9. Lim S, Naisbitt S, Yoon J, Hwang JI, Suh PG, Sheng M, et al. Characterization of the Shank family of synaptic proteins. multiple genes, alternative splicing, and differential expression in brain and development. J Biol Chem. 1999;274:29510–8.

10. Betancur C, Buxbaum JD. SHANK3 haploinsufficiency: a "common" but under-diagnosed highly penetrant monogenic cause of autism spectrum disorders. Mol Autism. 2013;4:17.

11. Durand CM, Betancur C, Boeckers TM, Bockmann J, Chaste P, Fauchereau F, et al. Mutations in the gene encoding the synaptic scaffolding protein SHANK3 are associated with autism spectrum disorders. Nat Genet. 2007;39:25–7.

12. Duffney LJ, Zhong P, Wei J, Matas E, Cheng J, Qin L, et al. Autism-like deficits in Shank3-deficient mice are rescued by targeting actin regulators. Cell Rep. 2015;11:1400–13.

13. Ma K, Qin L, Matas E Histone deacetylase inhibitor MS-275 restores social and synaptic function in a Shank3-deficient mouse model of autism. 2018; 43:1779–88.

14. Qin L, Ma K, Wang ZJ, Hu Z, Matas E, Wei J, et al. Social deficits in Shank3-deficient mouse models of autism are rescued by histone deacetylase (HDAC) inhibition. Nat Neurosci. 2018;21:564–75.

15. Qin L, Ma K, Yan Z. Chemogenetic activation of prefrontal cortex in Shank3-deficient mice ameliorates social deficits, NMDAR hypofunction, and Sgk2 downregulation. iScience. 2019;17:24–35.

16. Wang ZJ, Zhong P, Ma K, Seo JS, Yang F, Hu Z, et al. Amelioration of autism-like social deficits by targeting histone methyltransferases EHMT1/2 in Shank3-deficient mice. Mol Psychiatry. 2020;25:2517–33.

17. Yan Z, Rein B Mechanisms of synaptic transmission dysregulation in the prefrontal cortex: pathophysiological implications. Mol Psychiatry. 2021. https://doi: 10.1038/s41380-021-01092-3.

18. Shimazu T, Hirschey MD, Newman J, He W, Shirakawa K, Le Moan N, et al. Suppression of oxidative stress by beta-hydroxybutyrate, an endogenous histone deacetylase inhibitor. Science 2013;339:211–4.

19. Lee RWY, Corley MJ, Pang A, Arakaki G, Abbott L, Nishimoto M, et al. A modified ketogenic gluten-free diet with MCT improves behavior in children with autism spectrum disorder. Physiol Behav. 2018;188:205–11.

20. El-Rashidy O, El-Baz F, El-Gendy Y, Khalaf R, Reda D, Saad K. Ketogenic diet versus gluten free casein free diet in autistic children: a case-control study. Metab Brain Dis. 2017;32:1935–41.

21. Ahn Y, Narous M, Tobias R, Rho JM, Mychasiuk R. The ketogenic diet modifies social and metabolic alterations identified in the prenatal valproic acid model of autism spectrum disorder. Dev Neurosci. 2014;36:371–80.

22. Ruskin DN, Svedova J, Cote JL, Sandau U, Rho JM, Kawamura M Jr, et al. Ketogenic diet improves core symptoms of autism in BTBR mice. PLoS One. 2013;8:e65021.

23. Benjamin JS, Pilarowski GO, Carosso GA, Zhang L, Huso DL, Goff LA, et al. A ketogenic diet rescues hippocampal memory defects in a mouse model of Kabuki syndrome. Proc Natl Acad Sci USA. 2017;114:125–30.

24. Ruskin DN, Murphy MI, Slade SL, Masino SA. Ketogenic diet improves behaviors in a maternal immune activation model of autism spectrum disorder. PLoS One. 2017;12:e0171643.

25. Kouser M, Speed HE, Dewey CM, Reimers JM, Widman AJ, Gupta N, et al. Loss of predominant Shank3 isoforms results in hippocampus-dependent impairments in behavior and synaptic transmission. J Neurosci. 2013;33:18448–68.

26. Rein B, Ma K, Yan Z. A standardized social preference protocol for measuring social deficits in mouse models of autism. Nat Protoc. 2020;15:3464–77.

27. Hagelkruys A, Lagger S, Krahmer J, Leopoldi A, Artaker M, Pusch O, et al. A single allele of Hdac2 but not Hdac1 is sufficient for normal mouse brain development in the absence of its paralog. Development 2014;141:604–16.

28. Solomon MB. Evaluating social defeat as a model for psychopathology in adult female rodents. J Neurosci Res. 2017;95:763–76.

29. Bozdagi O, Sakurai T, Papapetrou D, Wang X, Dickstein DL, Takahashi N, et al. Haploinsufficiency of the autism-associated Shank3 gene leads to deficits in synaptic function, social interaction, and social communication. Mol Autism. 2010;1:15.

30. Jiang YH, Ehlers MD. Modeling autism by SHANK gene mutations in mice. Neuron 2013;78:8–27.

31. Peca J, Feliciano C, Ting JT, Wang W, Wells MF, Venkatraman TN, et al. Shank3 mutant mice display autistic-like behaviours and striatal dysfunction. Nature 2011;472:437–42.

32. Wang X, McCoy PA, Rodriguiz RM, Pan Y, Je HS, Roberts AC, et al. Synaptic dysfunction and abnormal behaviors in mice lacking major isoforms of Shank3. Hum Mol Genet. 2011;20:3093–108.

33. Wang X, Bey AL, Katz BM, Badea A, Kim N, David LK, et al. Altered mGluR5-Homer scaffolds and corticostriatal connectivity in a Shank3 complete knockout model of autism. Nat Commun. 2016;7:11459.

34. Speed HE, Kouser M, Xuan Z, Reimers JM, Ochoa CF, Gupta N, et al. Autism-associated insertion mutation (InsG) of Shank3 exon 21 causes impaired synaptic transmission and behavioral deficits. J Neurosci. 2015;35:9648–65.

35. Jaramillo TC, Speed HE, Xuan Z, Reimers JM, Liu S, Powell CM. Altered striatal synaptic function and abnormal behaviour in Shank3 exon4-9 deletion mouse model of autism. Autism Res. 2016;9:350–75.

36. Stoner R, Chow ML, Boyle MP, Sunkin SM, Mouton PR, Roy S, et al. Patches of disorganization in the neocortex of children with autism. N. Engl J Med. 2014;370:1209–19.

37. Bostock EC, Kirkby KC, Taylor BV. The current status of the ketogenic diet in psychiatry. Front Psychiatry. 2017;8:43.

38. Newman JC, Covarrubias AJ, Zhao M, Yu X, Gut P, Ng CP, et al. Ketogenic diet reduces midlife mortality and improves memory in aging mice. Cell Metab. 2017;26:547–57. e8

39. Roberts MN, Wallace MA, Tomilov AA, Zhou Z, Marcotte GR, Tran D, et al. A ketogenic diet extends longevity and healthspan in adult mice. Cell Metab. 2017;26:539–46. e5

40. Verpeut JL, DiCicco-Bloom E, Bello NT. Ketogenic diet exposure during the juvenile period increases social behaviors and forebrain neural activation in adult engrailed 2 null mice. Physiol Behav. 2016;161:90–98.

41. Newell C, Bomhof MR, Reimer RA, Hittel DS, Rho JM, Shearer J. Ketogenic diet modifies the gut microbiota in a murine model of autism spectrum disorder. Mol Autism. 2016;7:37.

42. Ahn Y, Sabouny R, Villa BR, Yee NC, Mychasiuk R, Uddin GM, et al. Aberrant mitochondrial morphology and function in the BTBR mouse model of autism is improved by two weeks of ketogenic diet. Int J Mol Sci. 2020;21:3266.

43. Smith J, Rho JM, Teskey GC. Ketogenic diet restores aberrant cortical motor maps and excitation-to-inhibition imbalance in the BTBR mouse model of autism spectrum disorder. Behav Brain Res. 2016;304:67–70.

44. Paoli A, Rubini A, Volek JS, Grimaldi KA. Beyond weight loss: a review of the therapeutic uses of very-low-carbohydrate (ketogenic) diets. Eur J Clin Nutr. 2013;67:789–96.

45. Zhang F, Rein B, Zhong P, Shwani T, Conrow-Graham M, Wang ZJ, et al. Synergistic inhibition of histone modifiers produces therapeutic effects in adult Shank3-deficient mice. Transl Psychiatry. 2021;11:99.

46. Guan JS, Haggarty SJ, Giacometti E, Dannenberg JH, Joseph N, Gao J, et al. HDAC2 negatively regulates memory formation and synaptic plasticity. Nature 2009;459:55–60.

47. Won H, Lee HR, Gee HY, Mah W, Kim JI, Lee J, et al. Autistic-like social behaviour in Shank2-mutant mice improved by restoring NMDA receptor function. Nature 2012;486:261–5.

48. Guo D, Peng Y, Wang L, Sun X, Wang X, Liang C, et al. Autism-like social deficit generated by Dock4 deficiency is rescued by restoration of Rac1 activity and NMDA receptor function. Mol Psychiatry. 2021;26:1505–19.

49. Rapanelli M, Tan T, Wang W, Wang X, Wang ZJ, Zhong P, et al. Behavioral, circuitry, and molecular aberrations by region-specific deficiency of the high-risk autism gene Cul3. Mol Psychiatry. 2021;26:1491–504.

AUTHOR CONTRIBUTIONS

L.Q. performed immunocytochemical, biochemical, electrophysiological experiments, analyzed data, and wrote the draft. K.M. performed behavioral experiments and analyzed data. Z.Y. designed experiments, supervised the project, and wrote the paper.

FUNDING

COMPETING INTERESTS
The authors declare no competing interests.

ADDITIONAL INFORMATION

Supplementary information The online version contains supplementary material available at https://doi.org/10.1038/s41386-021-01212-1.

Correspondence and requests for materials should be addressed to Zhen Yan.

Reprints and permission information is available at http://www.nature.com/reprints

Publisher's note Springer Nature remains neutral with regard to jurisdictional claims in published maps and institutional affiliations.